Quantitative structure-activity relationships for green algae growth inhibition by polymer particles

Nolte, T.; Peijnenburg, W.J.G.M.; Hendriks, A.J.; Meent, D. van de

Chemosphere 179 (2017) 49–56

Contents lists available at ScienceDirect

Chemosphere

journal homepage: www.elsevier.com/locate/chemosphere

Quantitative structure-activity relationships for green algae growth inhibition by polymer particles

Tom M. Nolte [a, *], Willie J.G.M. Peijnenburg [b], A. Jan. Hendriks [a], Dik van de Meent [b]

[a] Department of Environmental Science, Institute for Water and Wetland Research, Radboud University Nijmegen, P.O. Box 9010, 6500 GL Nijmegen, The Netherlands

[b] National Institute of Public Health and the Environment, P.O. Box 1, 3720 BA Bilthoven, The Netherlands

GRAPHICAL ABSTRACT

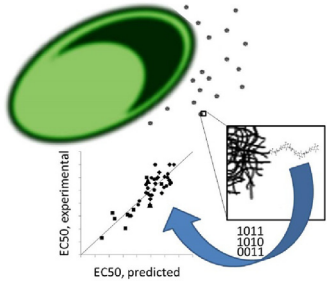

ARTICLE INFO

Article history:
Received 27 November 2016
Received in revised form
10 March 2017
Accepted 16 March 2017
Available online 19 March 2017

Handling Editor: Tamara S. Galloway

Keywords:
Algae
Growth inhibition
QSAR
Polymers
Molecular dynamics

ABSTRACT

After use and disposal of chemical products, many types of polymer particles end up in the aquatic environment with potential toxic effects to primary producers like green algae. In this study, we have developed Quantitative Structure-Activity Relationships (QSARs) for a set of highly structural diverse polymers which are capable to estimate green algae growth inhibition (EC50). The model (N = 43, R^2 = 0.73, RMSE = 0.28) is a regression-based decision tree using one structural descriptor for each of three polymer classes separated based on charge. The QSAR is applicable to linear homo polymers as well as copolymers and does not require information on the size of the polymer particle or underlying core material. Highly branched polymers, non-nitrogen cationic polymers and polymeric surfactants are not included in the model and thus cannot be evaluated. The model works best for cationic and non-ionic polymers for which cellular adsorption, disruption of the cell wall and photosynthesis inhibition were the mechanisms of action. For anionic polymers, specific properties of the polymer and test characteristics need to be known for detailed assessment. The data and QSAR results for anionic polymers, when combined with molecular dynamics simulations indicated that nutrient depletion is likely the dominant mode of toxicity. Nutrient depletion in turn, is determined by the non-linear interplay between polymer charge density and backbone flexibility.

1. Introduction

Use of chemical substances is regulated in various national and international legal frameworks. In Europe, chemicals can be marketed only if the tonnage is below a threshold of 1 tonne or after the

* Corresponding author.
E-mail address: tom.m.nolte@gmail.com (T.M. Nolte).

http://dx.doi.org/10.1016/j.chemosphere.2017.03.067

possibility of 'safe use' has been demonstrated in a REACH registration dossier (ECHA, 2012). 'Conventional' chemicals, such as polycyclic aromatic hydrocarbons (PAH) and other persistent organic pollutants (POPs) have been studied and evaluated extensively (Verbruggen, 2012); fate- and effect models exist to aid chemical safety analysis (Chen et al., 2006). For 'emerging pollutants', such models are available to a much lesser extent, particularly so for micro- and nano-sized particles (Braakhuis et al., 2015; Leszczynska and Shukla, 2009). While there are methods available that can estimate the effects of individual parent monomers (ECHA, 2012; Netzeva et al., 2007), the polymeric versions of the compounds are often left unevaluated. It is important to study the potential effects of nano- and micron-sized polymers because they represent a wider used class of potential pollutants. It is generally assumed that the increase in size relative to the monomer causes an overall decrease in toxicity (Congress 1983; Bergmann et al., 2009). However, this assumption was found incorrect for certain chemical species which exert higher toxicity than their individual constituents, like in the case of asbestos and cationic antimicrobial polymers (Boulanger et al., 2014; Uppu et al., 2016; Tsuji et al., 2006). Upon their release in the aquatic environment (Lambert and Wagner, 2016), nano and micro polymers have several potential detrimental effects on the ecosystem (Bergmann et al., 2009; da Costa et al., 2016). For example, bioconcentration or a loss in primary photosynthetic production by green algae may affect organisms higher up in the food chain (von Moos and Slaveykova, 2014; Khan and Arif, 2012; EFSA, 2016).

For chemicals that occur as nano- and micron-sized particles there are limited toxicological models available. Specifically, there is a lack of models for polymeric particles in the aquatic environment, with most of the models available developed for humans (Jagiello et al., 2016). Current modelling platforms like EPI Suite and ECOSAR (US EPA, 2012) include models predicting effects for algae, daphnia and fish for polymeric materials but have several important limitations. Datasets from which such models are derived are limited in size (and sometimes not publically available). Models are developed for specific polymer classes, i.e. cationics and anionics only, and can often give categorical classifications only (e.g. 'toxic' versus 'non-toxic') instead of quantitative estimations (US EPA, 2013). Due to these limitations, often no prediction is possible for a newly synthesized polymer since it does not conform the predetermined applicability domain or required input metric. For example, the only quantitative structure-activity relationship (QSAR) for algae toxicity available was developed by Boethling and Nabholz (Boethling and Nabholz, 1996), who found that the amine to polymer weight percentage (%A-N) correlated with green algae chronic toxicity. However, the equation did not apply above a certain threshold (%A-N > 3.5) for which chronic toxicity was found constant. Moreover, no statistical parameters were provided. For other polymer classes like non-ionics and anionics there exists much variance in algal toxicity data (Dědkova et al., 2014; van Hoecke et al., 2013; Boethling and Nabholz, 1996) and because there still exists uncertainty on the mechanisms by which they exert effect, it has not been possible to capture the variance into a model.

In theory, polymeric particles can exert toxicity in various ways. Polymeric materials >20 nm are unlikely to pass the cell wall of algae, but larger sized polymer particles can disrupt the cell wall, and cause photosynthesis inhibition (Navarro et al., 2008; Boethling and Nabholz, 1996; Bhattacharya et al., 2010). This is especially relevant in the case of cationic polymers since they electrostatically adsorb to cell walls and are subsequently able to react as nucleophiles in displacement reactions with various electrophilic moieties. In comparison, neutral and anionic polymers are usually less toxic and subtle effects could be explained by indirect shading (i.e. photosynthesis inhibition) or nutrient depletion through chelation (Nolte et al., 2016, Bhattacharya et al., 2010). For anionic polymers, chelation of cationic nutrients can be determined by measuring e.g. stability constants or complexation capacity (Wilson and Nicholson, 1993; Amjad, 2007), which are both highly dependent on chemical functionality. Since these potential modes of toxicity are driven for a large part by surface chemistry of the polymers, rather than surface area (Depan, 2016), we hypothesized that algae toxicity may be largely independent of particle size or underlying non-polymeric material. Therefore, in this study the aim was to develop mechanistically interpretable QSAR models for growth inhibition of green algae by a heterogeneous set of polymeric materials and polymeric coatings. Because the mode of action for anionic polymers is relatively uncertain, we also investigated the potential involvement of micro-nutrient depletion from the testing media. This was done by studying the conformational behaviour of anionic polymers in response to Mg^{2+} and Ca^{2+} ions using molecular dynamics. Subsequently, the information was used to explain some of the variance in the growth inhibition data.

2. Methods

2.1. Toxicity data

Data was collected from public literature using Google Scholar and Web of Science. Toxicity data were mostly 72-h growth inhibition EC50 values for freshwater green algae. However, since data was limited, marine algae species, 96-h growth-, and photosynthesis inhibition data were included as well. If both 96-h and 72-h EC50 data were available, the latter was used. Units were standardized to g/L and transformed logarithmically. No distinction was made between polymers of different sizes since this was not within our aim. The final data set contained algal toxicity data both for particles coated with polymers and pure polymer particles. If available, selection of compounds was limited to experiments using the actual exposure concentration (i.e. the suspended polymer) instead of the nominal concentration, thereby excluding highly hydrophobic polymers. Most growth inhibition tests were performed using OECD201 guidelines (OECD, 2011; van Hoecke et al., 2013; ECHA, 2012). For further details on the dataset see SI.

2.2. QSAR development

Custom 1D and 2D molecular descriptors were generated with RDKit using smiles input (RDKit, 2016). Polymer structures were drawn using Chemsketch (ACD/ChemSketch, 2013) and appropriate physiological (pH~7.4) charges attributed to each functional group. Unless mentioned otherwise, for each polymer eight repeating units were drawn and hydroxyl groups were added as termini, assuming radical polymerisation in aqueous media. In case of esterification and condensation, carboxylates and carbonyls were included as termini, respectively. Boethling and Nabholz (Boethling and Nabholz, 1996) did not provide structural representations of their polymers. Therefore, we estimated structural elements based on their detailed textual description (see SI). All the topological descriptors calculated were normalized using molecular weight. Correlation-based feature selection was used to extract relevant features from the pool of molecular descriptors. Subsequent feature selection was performed for the three distinct datasets separated based on the charge of the polymer. Charge carrying groups were amine and amidine (cationic), and carboxylic and sulfonic acid (anionic) groups. Pearson's correlation (R^2) coefficients, root mean square errors (RMSE) and p-values (at CI = 0.05) were determined using standard Python and Microsoft Excel statistical analysis packages (Anaconda, 2016).

2.3. Molecular dynamics

To investigate the potential role of micro-nutrient depletion on algal toxicity, we performed molecular dynamics (MD) simulations on the anionic polymers (poly)maleic acid (PMA) and (poly)acrylic acid (PAA) in association with magnesium and calcium ions. The standard 10 ns-long MD simulations of 25-chain long PMA and PAA at a ratio of 0.4 and 0.2 (0.4 and 0.2 divalent cations (Mg^{2+} and Ca^{2+}) per C(=O)O- unit) was performed in a similar way as (Assifaoui et al., 2015) which allowed for agglomeration of polymer chains in a cubic box model (Huynh et al., 2016). For more details, see SI. The relative immobilization of nutrient elements by the two polymers was expressed by the radius of gyration (R_g).

3. Results

3.1. QSAR

Correlation-based feature selection and linear regressions were performed for the full dataset and 'polymer class' datasets using the selected 2D descriptors generated using RDKit. Results are given in Table 1 and Fig. 1. Using the results for individual polymer classes, a decision tree (DT) (Puzyn et al., 2010) model was built.

3.2. Cationic polymers

The descriptor with highest correlation with observed algal toxicity was the total number of carbon-nitrogen bonds (#CN) of the nitrogen in the central amine (or amidine) functional group, normalized for polymer charge density. As the desirable number of data points per independent variable should be > 10–15 (Draper and Smith 1998; Frost, 2015; Tropsha, 2010) and the dataset for cationic polymers was small, no other polymeric descriptors were regarded potentially meaningful. The uniparameter QSAR for cationic amine and amidine polymers is:

$$-\log(EC_{50}) = -1.73 \times 10^{-2}\#CN + 5.78 \quad (N = 9,\ r^2 = 0.75,\ p = 3e-3) \tag{1}$$

3.3. Neutral polymers

The IPC index, normalized for molecular weight, explains most of the variance in the observed endpoint being positively correlated with algae toxicity to neutral polymers (Table 1). The IPC index is the information content of the coefficients of the characteristic polynomial of the adjacency matrix of a hydrogen-suppressed graph of a molecule (Bonchev and Trinajstic, 1977). An adjacency matrix is a square matrix used to represent a finite graph. The elements of the matrix indicate whether pairs of vertices (i.e. atoms) in the graph are adjacent and what the distribution of distances is. Effectively, the IPC index quantifies the 'structural complexity' of the polymers (Avula et al., 1983; Bonchev and Trinajstic, 1977) (Fig. 2). One outlier (ID = N14, see SI) was removed from the original dataset (N = 19) as this was a polymeric surfactant not adhering to the linear IPC graph representation due to its tertiary structure in aquo.

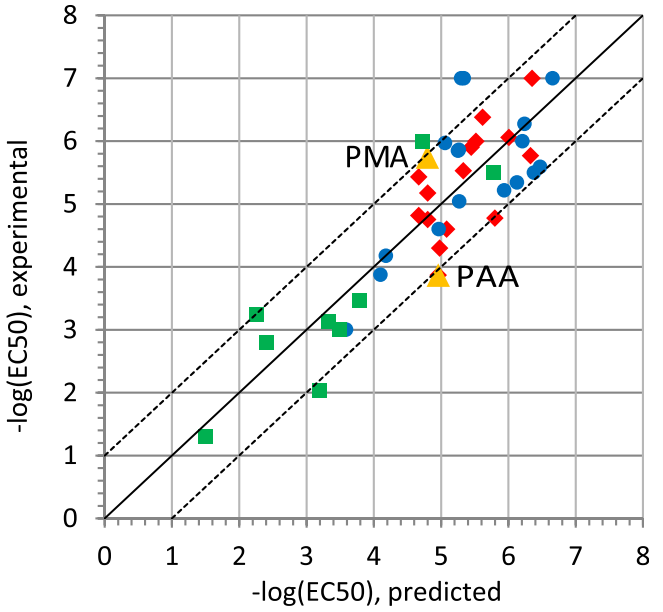

Fig. 1. Graphical representation of the decision tree QSAR using 1 polymeric descriptor for each polymer class, i.e. #CN, IPC and PEOE_VSA9 ($R^2 = 0.73$; RMSE = 0.28). Cationic (green squares); non-ionic (blue circles); anionic (red diamonds). Two outliers, polymaleic acid (PMA) and polyacrylic acid (PAA) are shown separately (yellow triangles). log(EC50) in g/L. (For interpretation of the references to colour in this figure legend, the reader is referred to the web version of this article.)

Apart from the IPC index, SlogP_VSA3 showed a significant inverse correlation. SlogP_VSA3 is a subdivided surface area descriptor based on the all-atom summation of the approximate accessible van der Waal's surface area with contribution to the partition coefficient (octanol/water). Here it is calculated for each atom with polarities in the range of 0–0.1 and can be regarded as a measure for hydrophobicity (Wildman and Crippen, 1999; Labute, 2000). The uniparameter QSAR for non-ionic polymers is:

$$-\log(EC_{50}) = -1.43 \times 10^{-1} IPC + 6.88 \quad (N = 17,\ r^2 = 0.60,\ p = 3e-4) \tag{2}$$

Table 1
Polymeric descriptors identified using correlation-based feature selection.

Polymer type	Cationic (N = 9) LR	Non-ionic (N = 17) LR	Anionic (N = 16) LR	Full dataset (N = 43) MLR[b]	Full dataset (N = 43) Decision tree[c]
Descriptor[a]:	#CN: $R^2 = 0.75$ $p = 0.003$	IPC index: $R^2 = 0.60$ $p < 0.001$	PEOE_VSA9: $R^2 = 0.46$ $p = 0.005$	#CN;PEOE_VSA12; Kappa3: $R^2 = 0.64$	#CN; IPC; PEOE_VSA9: $R^2 = 0.73$
Descriptor[a]:	N/A	SlogP_VSA3: $R^2 = 0.49$ $p = 0.002$	Hall&Kier index: $R^2 = 0.44$ $p = 0.007$	N/A	N/A

[a] #CN: normalized number of carbon-nitrogen bonds on the central nitrogen; IPC index: information for polynomial coefficients based information theory; PEOE_VSA9: MOE-type descriptor using partial charges and surface area contributions; SlogP_VSA3: MOE-type descriptor using SLogP and surface area contributions; Hall&Kier index: Kier and Hall valence connectivity index.
[b] The MLR QSAR developed was: $\log(EC_{50}) = -1.54 \times 10^2$ #CN + 1.75×10^1 PEOE_VSA12 + 1.66×10^1 Kappa3 + 4.76.
[c] See also Fig. 1 for a graphical representation of the DT QSAR.

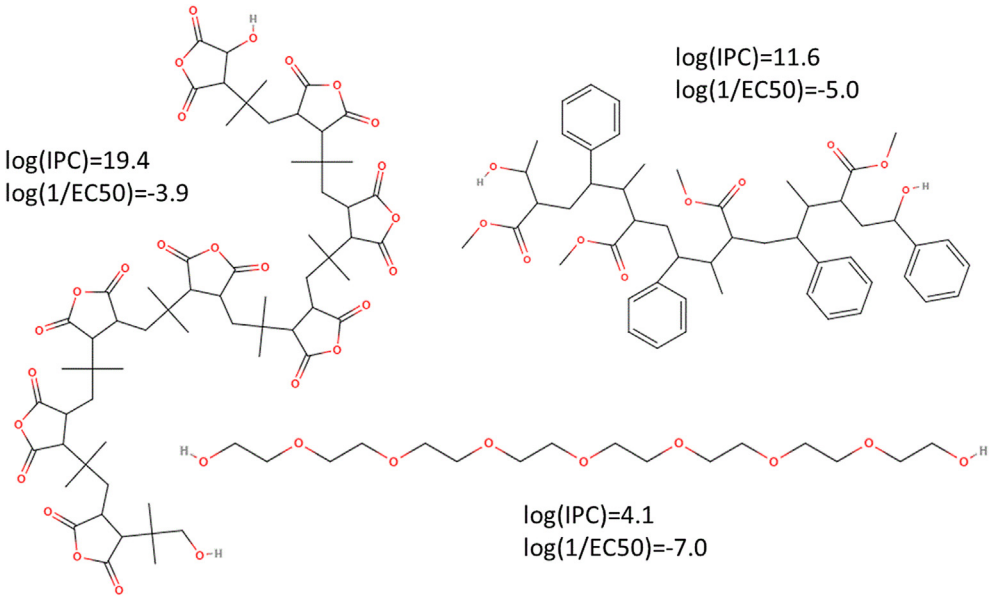

Fig. 2. The MW-normalized IPC index calculated for three neutral polymer segments and corresponding algal toxicity.

3.4. Anionic polymers

The 2D descriptor with highest correlation was PEOE_VSA9, which is a MOE-type descriptor using partial charges and surface area contributions and captures direct electrostatic interactions (Labute, 2000). The outlier poly(maleic acid) was removed from the original dataset (N = 17) because of its high charge density (−0.24 per heavy atom) (Lyklema, 2005; Koper and Borkovec 2010) and its behaviour was further investigated using molecular dynamics. The Kier&Hall molecular connectivity index (normalized for polymer weight) was weakly positively associated with algal toxicity to anionic polymers. The Hall&Kier index (χ) is a series of numbers designated by "order" and "subgraph type." The subgraph types path, cluster and chain emphasize different aspects of atom connectivity within a polymer, for example, the amount of ring branching and flexibility (Kier and Hall, 1976). The uniparameter QSAR for anionic polymers is:

$$-\log(EC_{50}) = 2.39 \times 10^{-2} PEOE_{VSA9} + 4.58{*}10^{-1} \quad (3)$$
$$(N = 16,\ r^2 = 0.46,\ p = 5e-3)$$

3.5. Combination of model classes

Multi linear regression using 2D descriptors on the entire dataset (N = 44) gave poor model performance, see Table 1. The descriptor with highest relevance was POE_VSA9. Because of the poor model performance, instead the three model classes (Eqs. (1)–(3)) were combined using a decision tree, generating a satisfactory model (Table 1). In this model >90% of the predictions were within 1 order of magnitude, see Fig. 1.

3.6. Molecular dynamics simulation

The nutrient cations Ca^{2+} and Mg^{2+} show affinity to both the PAA and PMA oligomers, see Fig. SI2. In response to the association of Ca^{2+} and Mg^{2+} the radii of gyration of all oligomer complexes decreased over time, though the effect was more significant for PAA oligomers, see Fig. 2. R_g is a measure of compactness and stability of a polyeletrolyte complex (Tadros, 2015), and its relative decrease for PAA compared to PMA indicates that PAA is more prone to immobilize cationic nutrients. The relative order of stability was PAA/Ca^{2+} > PAA/Mg^{2+} > PMA/Ca^{2+} > PMA/Mg^{2+}. The average persistence lengths, a measure for the stiffness of a polymer, of 25 monomers stayed relatively constant over the course of 10 ns simulations and were 9, 7, 25 and 29 for PAA/Ca^{2+}, PAA/Mg^{2+}, PMA/Ca^{2+} and PMA/Mg^{2+}, respectively (SI).

4. Discussion

4.1. General

Several important limitations of the model developed are apparent and are mostly due to the internal variability in the dataset from the open literature. Firstly, data for different algal species, e.g. *P. subcapitata* and *Chlorella sp.*, was combined. Such algae species may have different sensitivities towards synthetic polymers due to differences in metabolism, nutrient requirements and physiology (Singh and Singh, 2015; Domozych et al., 2012; Fogg et al., 1973). Interestingly, when algae species other than *P. subcapitata* were excluded from the non-ionic polymer dataset model performance improved (R^2 = 0.72, N = 9). However, interspecies differences are relatively small compared to absolute polymer toxicity (Finkle and Appleman, 1953; Goecke et al., 2015; Noro, 1985; Boethling and Nabholz, 1996; Fu et al., 2015), and interspecies difference in PVP toxicity was within 1 order of magnitude (see Table SI2). Secondly, particle sizes were in the range 20 < d < 200, but larger particles were likely also included (SI). Generally, toxicity decreases with size which is linked to the decrease of (reactive) surface area. For instance, for inorganic nanoparticles, a factor ~2 for CeO_2-14 compared to CeO_2-29 (72h EC50) (Van Hoecke et al., 2009), and a factor ~5 for nZVI-20 compared to nZVI-100 (96h IC50) (Lei et al., 2016) have been observed. When expressing the concentration in surface area (m^2/L), van Hoecke et al. found no significant difference in toxicity by either SiO_2 or CeO_2 (Van Hoecke et al., 2008, 2009). The combined results indicate that more robust polymer-QSARs can be developed using new data expressed in m^2/L. Also, media chemistry (e.g. pH, ionic strength) (Zamani et al., 2014), exposure regime (effective

suspended vs. nominal conc.) and duration (Casado et al., 2013) can result in discrepancies for a tested polymer in different conditions as this influences test outcomes in non-linear ways. For example, added nutrients complex with anionic polymers whereas dissolved organic carbon (DOC) mitigates the aquatic toxicity of cationic polymers (Boethling and Nabholz 1996). To date, only few methods exist to predict the influence of media chemistry on toxicity by nanoparticles (Nolte et al., 2015; Van Hoecke et al., 2011).

Apart from the variability discussed above, there is also uncertainty in our dataset (Table SI1) as for 8 of the 44 polymers we either needed to estimate the repeating unit or the distribution within the polymer as there was only textual information available on the polymeric structures. In theory, this can introduce errors in the calculations of the descriptors used, e.g. an incorrect number of carbons in a side chain or branching in the polymer. Specifically, we estimated the distribution of the monomers based on a polymer segment consisting of 8 repeating units and it was assumed that this segment is repetitive for the entire polymer while this may not be the case. However, most of the structures estimated are reasonable estimates based on basic polymer chemistry (Wilson and Nicholson, 1993; Young and Lovell 2011), and the fact that textual descriptions in publications are detailed (Boethling and Nabholz 1996). Moreover, it was known what chemical functionalities the polymer had. Some of the polymers used were coatings on metal (oxide) nanoparticles but pooling this data (factor difference <3 for HASE and starch polymers) is justified since these underlying materials are inert (e.g. gold, PbS), see SI.

When using the total dataset (N = 43), conventional multiple linear regression using three 2D descriptors led to moderate predictions of algal polymer toxicity (Table 1). Multi linear regression on the total dataset was unsuccessful because the method is not suitable to deal with such diverse chemical structures in the relatively small dataset. Class-specific models performed substantially better, and thus a decision tree could be used to combine models for individual polymer classes, improving overall performance (Fig. 1). From our QSAR analysis we identified several descriptors that correlate with algal toxicity (Table 1). Applications of QSAR/QSPR approaches to estimate polymer properties typically use similar descriptors derived for repeating units, such as molecular weight of a repeating unit, end-to-end distance, van der Waals volumes, charged partial surface areas, topological indices, and cohesive energy (Bicerano, 2002; Seitz, 1993). Because of the wide use of these descriptors, it is likely that they represent a wider range of properties including algal toxicity. Common modelling validation practice (>10–15 data points per independent descriptor) (Draper and Smith 1998; Frost, 2015; Tropsha, 2010) indicates that the two-parameter models are not desirable. However, all descriptors identified (Table 1) have mechanistic interpretations which are discussed in the next sections.

4.2. Cationic polymers

The model developed for cationic polymers gives quantitative estimations for algal toxicity using the number of C–N bonds (#CN) as a single generic descriptor. We were unable to compare the developed model to a previous model developed by Boethling and Nabholz (Boethling and Nabholz, 1996) for chronic algal toxicity because no detailed structural information or statistical parameters were provided: log[Green Algae ChV] = 1.057–1 × %A-N (with %A-N representing the amine to polymer weight percentage). However, both the previous and newly developed model reflect the same potential modes of toxicity. The limited data used (N = 9) did not allow generating a statistically robust QSAR for cationic polymers (Draper and Smith 1998; Frost, 2015; Tropsha, 2010). However, the descriptor selected (#CN) strongly relates to the mode of toxicity, underpinning its validity. All polymers were linear except 1 (PAMAM) but limited influence due to branching (backbone architecture) needs to be expected (Costa et al., 2014).

It is generally agreed upon that cationic particles affect algae through adsorption on and/or disruption of the outer cell wall. The cell walls of green algae contain assemblages of polymers including cellulose, pectins, hemicelluloses, arabinogalactan proteins (AGPs), extension, and lignin (Domozych et al., 2012). These structural elements contain hydroxyl and carboxyl groups giving the cell wall its anionic character attracting cationic amine and amidine polymers. Moreover, polymeric amines and amidines can participate as nucleophiles in displacement reactions with electrophilic carbonyl functionalities present in the algal cell wall. Secondary amines (R_2NH) are usually less reactive than primary amines (RNH_2) because of steric hindrance by the hydrocarbon groups reducing the ability of an incoming reactant molecule to interact with the central nitrogen atom. The reactivity of amines as nucleophiles and imine formation depends upon the presence of a free electron pair on nitrogen, and therefore, quaternary ammonium polymers (R_4N^+) do not undergo such reactions and are relatively inert (IUPAC, 2014). Also, because they exist as permanent cations, they do not diffuse readily across biological membranes. The precise reactivity of amines (and amidines) and electrostatic attraction of quaternary ammonium compounds depends on local steric influences and resonance effects, which in turn may also be induced by conformational changes of the polymer (Young and Lovell, 2011). Currently there is insufficient data to such select such descriptors and develop a model able to distinguish between and quantify the different modes by which cationic polymers can exert toxicity to algae.

4.3. Neutral polymers

Feature selection and linear regression indicated that the IPC index, which quantifies 'structural complexity', is the most relevant theoretical descriptor. It is known that the amount of branching in a polymer can increase toxicity, as well as the introduction of electrophilic functional groups like aldehydes, anhydrides and conjugated double bonds (Kaur et al., 2016; Kafil and Omidi, 2011; Wilson and Nicholson, 1993; Boethling and Nabholz, 1996) (Fig. 2). The highest algal growth inhibition for a neutral polymer in our dataset was found for poly(isobutylene-*alt*-maleic anhydride) (PIAM) (Van Hoecke et al., 2011), and accordingly this polymer has a high IPC index, Fig. 2. PIAM can act as a nucleophile in ring opening and closure reactions which can interfere with nucleophilic substitution catalysed by enzymes *in vivo* (Bortel and Stysło, 1990).

SlogP_VSA3 which represents the accessible van der Waal's surface area and hydrophobicity was found to describe toxicity as well. Non-ionic polymers are generally of low concern for aquatic hazard. However, hydrophobic polymers or residues may absorb through or disrupt the thylakoid membrane, but they would need to pass the algal cell wall (pore size ~20 nm) (Navarro et al., 2008). Polymers which have Mw > 1000 kD are not expected to be absorbed through biological membranes and it is more likely that they exert toxicity by affecting the outer cell wall of algae. In case of highly agglomerating polymers, hydrophobicity can also inhibit photosynthesis via shading. Non-ionic polymers that have monomers grouped in such a way that it exerts surfactant or dispersant properties, cause excessive toxicity to aquatic organisms. This is clearly the case for the triblock copolymer poloxamer (ID = N14, see SI) which has an amphiphilic structure and showed a high algal toxicity compared to model prediction. This clearly shows that the developed model is not suitable for polymeric surfactants, for which other QSARs exist (Mayo-Bean et al., 2012).

4.4. Anionic polymers

Previous studies showed that a potential toxic mode of action for many (poly)carboxylic acids is complexation of nutrient elements needed by algae for growth (Boethling and Nabholz 1996). Secondary effects like shading may also affect growth by directly inhibiting photosynthesis (Hartmann et al., 2013; Bhattacharya et al., 2010). However, it is less likely for the polymers in this study since they are mostly non-agglomerated suspensions. Moreover, effect concentrations for anionic polymers are relatively low and photosynthesis wavelengths do not fully overlap with absorption/scattering wavelengths of polymers (Nolte et al., 2016). The descriptors selected using QSAR modelling reflect the polymer properties influencing cation binding and the main mode of toxic action (i.e. nutrient depletion). The 2D descriptors PEOE_VSA9 and the Hall&Kier index capture direct electrostatic interactions as well as branching and flexibility, which are related to the polymers ability to complex and/or chelate nutrient elements (Duca and Hopfinger 1999).

Macronutrients that algae need are nitrogen, phosphorus, sulfur, carbon, magnesium and calcium. Of these only magnesium and calcium can chelate with (poly)carboxylic acids. Effects of algal micro-nutrient deficiencies have widely been reported. For example, Mg deficiency ($\leq$2.8 ppm) interrupted cell multiplication and reduced photosynthetic activity of the PSII system (about 20%) in *C. vulgaris* (Finkle and Appleman, 1953) and the absence of Mg^{2+} decreased algal Chl content by 60% and reduced photosynthetic activity of the PSII system by 24% in C. reinhardtii (Volgusheva et al., 2015). In Ca^{2+} deficient conditions, photosynthetic oxygen evolution, growth rate and chlorophyll content are affected (Adam and Issa, 2000). Ca^{2+} and Mn^{2+} also exist in the oxygen-evolving complex of algal PSII as water oxidation takes place at a catalytic Mn(4)-Ca site, which is embedded in the thylakoid membrane (Yachandra and Yano, 2011; Hou and Hou, 2013). Very similar effects, i.e. photosynthesis inhibition and decrease in PSII activity, have been reported for *P. subcapitata* and *C. reinhardtii* exposed to carboxylate-functionalized polystyrene and (poly)styrene-co-butyl acrylate, for which growth inhibition data was included in our dataset (Table SI1). Of the complexation constants of PAA for nutrient elements discussed, by far the highest was found for Mn^{2+}, see Table 2 (Wilson and Nicholson, 1993). Other trace elements might also be relevant, and it is difficult to assess which nutrient element is the limiting factor. From existing data, it seems apparent that chelation of Mn^{2+} may be the most important factor for PAA toxicity, while there may also be synergetic and antagonistic effects involving other nutrients (Fogg et al., 1973; Singh and Singh, 2015).

Effect levels for anionic polymers vary more than 2 orders of magnitude, with e.g. the EC50's for PAA and PMA 7.44 and 560 mg/L, respectively (Table SI1). The effect level for PAA corresponds to 3.2 mmol/L carboxylate groups. Consequently, upon addition of PAA the calculated free concentration of nutrients in the growth medium (see SI) is far lower compared to ideal growth conditions [OECD201, 2011] (Table 2). PAA is moderately toxic to algae and it appeared to be the most potent (poly)carboxylic acid regarding its ability to chelate nutrients (Boethling and Nabholz, 1996), Table 2. This however, is counterintuitive since PMA (an outlier in our model, see Fig. 1) exerts low toxicity even though it has twice as much carboxylate density on the polymer backbone, especially since it was shown that the introduction of maleic acid monomers significantly increases the calcium binding capacity of PAA polymers (Serin et al., 2013). Apart from charge density and distribution, the extent and rate of interaction between hydrated counter ions and polyanions also depends on polymer structure and conformation, acid strength, and the degree of dissociation of the polymer chain. Weak anionic polyelectrolytes undergo conformational changes, depending on the system pH and salinity. Generally, the strength of ion binding is enhanced when the arrangements of the functional groups permit chelate formation (Wilson and Nicholson, 1993). While PMA has a higher cation binding capacity than PAA, this does not directly imply that more cations are bound. Stabilization (%) of d-block metals (Fe^{3+} and Mn^{2+} investigated) in the presence of 20 ppm polymers containing C(=O)O- groups was 62% for polyacrylic acid (PAA) and 65% for polymethacrylic acid but only 4% for polymaleic acid (PMA) (Amjad, 2007).

4.5. Molecular dynamics simulation

It was observed that Mg^{2+} and Ca^{2+} electrostatically interact with both PAA and PMA. The radius of gyration (Fig. 3) of PAA

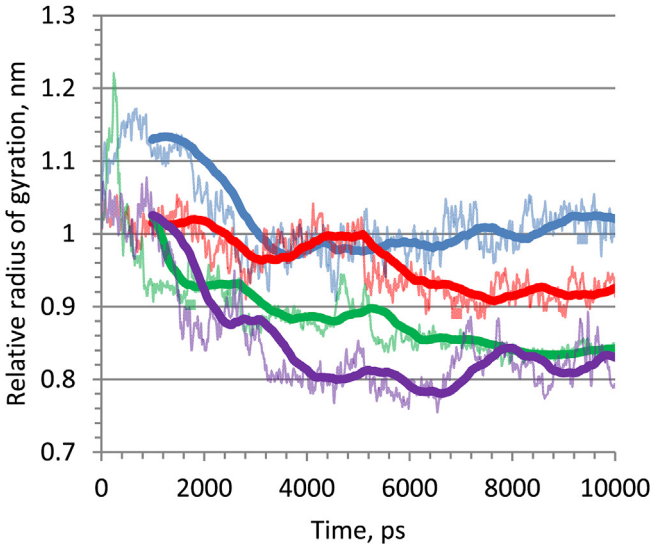

Fig. 3. The evolution of the radius of gyration of polymaleic acid (PMA) and polyacrylicic acid (PAA) during a 10-ns equilibration in the presence of 10 Ca^{2+} and 10 Mg^{2+} ions. Blue: PMA/Mg^{2+}, red: PMA/Ca^{2+}, green: PAA/Mg^{2+}, purple: PAA/Ca^{2+}. Dark data series denote moving averages of 1 ns. (For interpretation of the references to colour in this figure legend, the reader is referred to the web version of this article.)

Table 2
Elemental nutrient requirements of green algae, concentrations in OECD201 tests, and complexation constants with poly(acrylic acid), PAA.

Nutrient element	Optimal algal growth levels, mmol/L	OECD algal growth test concentration, mmol/L[d]	PAA complexation constant[e]
Mg^{2+}	0.1–1.7 (2.8–49 mg/L)[a]	0.1 (2.9 mg/L)	6.0×10^1
Ca^{2+}	~0.05 (~2.4 mg/L)[b]	0.1 (4.9 mg/L)	1.0×10^2
Mn^{2+}	0.002–0.02 (0.1–1.0 mg/L)[c]	0.002 (0.115 mg/L)	2.3×10^3

[a] For *C. vulgaris* [Finkle and Appleman, 1953].
[b] For D. quadricauda [Goecke et al., 2015].
[c] For D. tertiolecta [Noro, 1985].
[d] [OECD201, 2011].
[e] [Wilson and Nicholson, 1993].

decreases significantly with the addition of Ca^{2+} and Mg^{2+} due to chelation and complexation. While chelation of Ca^{2+} occurred for both PMA and PAA, chelation of Ca^{2+} (as well as complexation of Mg^{2+}) by PMA only slightly affected the radius of gyration of the PMA polymer. Moreover the persistence lengths of PMA polymers were high (SI). This strongly implies that PMA is not as flexible as was quantified using the Hall&Kier index (χ). Under alkaline conditions, electrostatic forces are strong enough to break the intramolecular cohesion due to deprotonation of carboxylic groups on PAA and PMA (e.g. $\theta \geq 0.2$ for PMAA) (Lyklema, 2005) leading to stretching of polymer backbones and good solubility. This was reproduced by simulations for fully deprotonated PMA and PAA in pure water (Fig. SI2). In contrast to PAA, the backbone of PMA assumes a near linear conformation to minimize its internal electrostatic potential, even in high cation concentrations (Fig. 2). This supports literature data for PAA which is a spherical ball in unionized form, but is a winding chain in ionized form (Jacobson 1962). Since, in monovalent solutions, the fraction charged on PMA (5 < pKa <7 (Sigrid et al., 2010)) is only slightly lower than on PAA (pKa~4.2 (Cesarano et al., 1988; Gebhardt and Fuerstenau, 1983)), protonation (θ_{PAA}~0.8 (Koper and Borkovec, 2010) and θ_{PMA}~0.5 (Lyklema, 2005; Koper and Borkovec 2010) at pH~7.5) alone cannot explain the near-two orders of magnitude difference in algal toxicity between PMA and PAA (Fig. 1, Table SI1). The performance of the QSAR model for anionic polymers was not satisfactory (Table 1, Equation (3)), and it is hypothesized that the interplay between polymer charge density and flexibility causes non-linearity between the descriptors used (i.e. the Hall&Kier index, χ) and algal toxicity. Our molecular dynamics study demonstrates that carboxylate polymer flexibility is dependent not only on the number of rotatable bonds but also charge on the backbone. As a result, nutrient binding is enhanced by physical immobilization due to chelation and complexation (PAA), but too high charge on the backbone limits nutrient stabilization due to short-range self-repulsion, i.e. the loss of polymer flexibility (PMA). Polymer properties such as the electrostatic persistence length may be able to better capture the effect of nutrient depletion on algal toxicity (Ullner et al., 1997; Cranford and Buehler, 2012). Whether nutrient depletion can be achieved under field conditions depends on the relative concentrations of both the nutrient levels and polymeric functional groups introduced. However since the absolute volume of nutrients is relatively large, minimal algal toxicity should be expected in the field.

5. Conclusion

We have developed QSARs for highly structurally diverse polymers which are capable to estimate green algae toxicity (EC50) within 1 order of magnitude, independent of polymer particle size and underlying inorganic core material. The models may be applied in risk assessment and are applicable for linear homo polymers as well as copolymers. The model performs best for cationic and non-ionic polymers with 20 < d < 200 nm while for anionic polymers specific properties of the polymer and test conditions need to be known for further evaluation. Highly branched polymers, non-nitrogen cationic polymers and polymeric surfactants are not included in the model and thus cannot be evaluated. In the future, new growth inhibition data for specific algal species using more appropriate dose metrics will aid to support advanced modelling techniques using decision trees, 3D descriptors and molecular dynamics simulations.

Appendix A. Supplementary data

Supplementary data related to this article can be found at http://dx.doi.org/10.1016/j.chemosphere.2017.03.067.

References

ACD/Labs, 2013. ACD/Chemsketch for Academic and Personal Use. http://www.acdlabs.com.

Adam, M.S., Issa, A.A., 2000. Effect of manganese and calcium deficiency on the growth and oxygen exchange of scenedesmus intermedius cultured for successive generations. Folia Microbiol. 45 (4), 353–358.

Amjad, Z., 2007. Influence of polymer architecture on the stabilization of iron and manganese ions in aqueous systems. Tenside Surf. Det. 44, 4.

Anaconda Software Distribution, Nov. 2016. Computer Software. Vers. 2-2.4.0. Continuum Analytics. Web. https://continuum.io.

Assifaoui, A., Lerbret, A., Uyen, H.T.D., Neiers, F., Chambin, O., Loupiac, C., Cousin, F., 2015. Structural behaviour differences in low methoxy pectin solutions in the presence of divalent cations (Ca2+ and Zn2+): a process driven by the binding mechanism of the cation with the galacturonate unit. Soft Matter 11, 551–560.

Avula, X.J.R., Kalman, R.E., Liapis, A.I., Rodin, E.Y., 1983. Mathematical Modelling in Science and Technology: Neighbourhood Complexities and Symmetry of Chemical Graphs and Their Biological Applications. Pergamon Press, pp. 745–750.

Bergmann, M., Gutow, L., Klages, M., 2009. Marine Anthropogenic Litter: Chapter 10. Microplastics in the Marine Environment: Distribution, Interactions and Effects. Springer Open.

Bhattacharya, P., Lin, S., Turner, J.P., Ke, P.V., 2010. Physical adsorption of charged plastic nanoparticles affects algal photosynthesis. J. Phys. Chem. C 114, 16556–16561.

Bicerano, J., 2002. Prediction of Polymer Properties, third ed. Marcel Dekker Inc, New York, USA.

Boethling, R.S., Nabholz, J.V., 1996. Environmental assessment of polymers under the U.S. Toxic substances control act. In: Hamilton, J.D., Sutcliffe, R. (Eds.), Ecological Assessment of Polymers Strategies for Product Stewardship and Regulatory Programs. Van Nostrand Reinhold, New York, pp. 187–234.

Bonchev, D., Trinajstic, N., 1977. Information theory, distance matrix, and molecular branching. J. Chem. Phys. 67, 4517.

Bortel, E., Stysło, M., 1990. On the chemical modifications of poly(maleic anhydride-co-isobutene) by means of hydrolysis, ammoniation or aminations. Macromol. Chem. Phys. 191 (11), 2653–2662.

Boulanger, G., Andujar, P., Pairon, J., Billon-Galland, M., Dion, C., Dumortier, P., Brochard, P., Sobaszek, A., Bartsch, P., Paris, C., Jaurand, M., 2014. Quantification of short and long asbestos fibers to assess asbestos exposure: a review of fiber size toxicity. Environ. Health 13, 59.

Braakhuis, H.M., Kloet, S.K., Kezic, S., Kuper, F., Park, M.V.D.Z., Bellmann, S., van der Zande, M., Le Gac, S., Krystek, P., Peters, R.J.B., Rietjens, I.M.C.M., Bouwmeester, H., 2015. Progress and future of in vitro models to study translocation of nanoparticles. Arch. Toxicol. 89, 1469–1495.

Casado, M.P., Macken, A., Byrne, H.J., 2013. Ecotoxicological assessment of silica and polystyrene nanoparticles assessed by a multitrophic test battery. Environ. Int. 51, 97–105.

Cesarano, J., Aksay, I.A., Bleier, A., 1988. Stability of a-Al2O3 suspensions with polymethacrylic acid polyeletrolyrte. J. Am. Ceram. Soc. 71, 250–255.

Chen, C.Y., Yan, Y.K., Yang, C.F., 2006. Toxicity assessment of polycyclic aromatic hydrocarbons using an air-tight algal toxicity test. Water Sci. Technol. 54 (11–12), 309–315.

Congress of the U.S. Office of Technology Assessment, 1983. The Information Content of Premanufacture Notices: Background Paper: Chapter 6. Frequency of Submission of Toxicity Information on Premanufacture Notices. University of Michigan Library, Washington D.C.

Costa, R., Pereira, J.L., Gomes, J., Gonçalves, F., Hunkeler, D., Rasteiro, M.G., 2014. The effects of acrylamide polyelectrolytes on aquatic organisms: relating toxicity to chain architecture. Chemosphere 112, 177–184.

Cranford, S.W., Buehler, M.J., 2012. Variation of weak polyelectrolyte persistence length through an electrostatic contour length. Macromolecules 45, 8067–8082.

da Costa, J.P., Santos, P.S., Duarte, A.C., Rocha-Santos, T., 2016. (Nano)plastics in the environment - sources, fates and effects. Sci. Total Environ. 1 (566–567), 15–26.

Depan, D., 2016. Biodegradable Polymeric Nanocomposites. Advances in Biomedical Applications: Chapter 9: Plastics of the Future. Innovations for Improvement and Sustainability with Special Relevance to Biomedical Applications. CRC Press, Boca Raton, FL.

Domozych, D.S., Ciancia, M., Fangel, J.U., Mikkelsen, M.D., Ulvskov, P., Willats, W.G.T., 2012. The cell walls of green algae: a journey through evolution and diversity. Front. Plant Sci. 3, 82.

Draper, N.R., Smith, H., 1998. Applied Regression Analysis, third ed. Wiley, New York, USA.

Duca, J.S., Hopfinger, A.J., 1999. Molecular modeling of polymers 18. Molecular dynamics simulation of poly(acrylic acid) copolymer analogs. Capture of calcium ions as a function of monomer structure, sequence and flexibility. Comput. Theor. Polym. Sci. 9 (3–4), 227–244.

Dědkova, K., Bures, Z., Palarčik, J., Vlček, M., Kukutschová, J., 2014. Acute Aquatic Toxicity of Gold Nanoparticles to Freshwater Green Algae. NanoCon 2014 Brno, Czech Republic.

ECHA European Chemicals Agency, 2012. Guidance on Registration. Version 2.0. Guidance for the Implementation of REACH.

EFSA Panel on Contaminants in the Food Chain (CONTAM), 2016. Presence of microplastics and nanoplastics in food, with particular focus on seafood. EFSA J. 14 (6), 4501.
Finkle, B.J., Appleman, D., 1953. The effect of magnesium concentration on growth of Chlorella. Plant Physiol. 28 (4), 664–673.
Fogg, G.E., Stewart, W.D.P., Fay, P., Walsby, A.E., 1973. The Blue-green Algae. Academic Press, London, UK.
Frost, J., 2015. The Danger of Overfitting Regression Models. http://blog.minitab.com. Retrieved 2016-07-31.
Fu, L., Li, J.J., Wang, Y., Wang, X.H., Wen, Y., Qin, W.C., Su, L.M., Zhao, Y.H., 2015. Evaluation of toxicity data to green algae and relationship with hydrophobicity. Chemosphere 120, 16–22.
Gebhardt, J.E., Fuerstenau, D.W., 1983. Adsorption of polyacrylic acid at oxide/water interfaces. Colloids Surf. 7, 221–231.
Goecke, F., Jerez, C.G., Zachleder, V., Figueroa, F.L., Bišová, K., Rezanka, T., Vítová, M., 2015. Use of lanthanides to alleviate the effects of metal ion deficiency in Desmodes musquadricauda (Sphaeropleales, Chlorophyta). Front. Microbiol. 6 (1).
Hartmann, N.B., Engelbrekt, C., Zhang, J., Ulstrup, J., Kusk, K.O., Baun, A., 2013. The challenges of testing metal and metal oxide nanoparticles in algal bioassays: titanium dioxide and gold nanoparticles as case studies. Nanotoxicology 7 (6), 1082–1094.
Hou, X., Hou, H.J.M., 2013. Roles of manganese in photosystem II dynamics to irradiations and temperatures. Front. Biol. 8, 312–322.
Huynh, U.T.D., Lerbret, A., Neiers, F., Chambin, O., Assifaoui, 2016. Binding of divalent cations to polygalacturonate: a mechanism driven by the hydration water. J. Phys. Chem. 120, 1021–1032.
IUPAC International Union of Pure and Applied Chemistry, 2014. Compendium of Chemical Terminology Gold Book. Version 2.3.3.
Jacobson, A.D., 1962. Configurational effects on binding of magnesium to polyacrylic acid. J. Polym. Sci. 57, 321–336.
Jagiello, K., Grzonkowska, M., Swirog, M., Ahmed, L., Rasulev, B., Avramopoulos, A., Papadopoulos, M.G., Leszczynski, J., Puzyn, T., 2016. Advantages and limitations of classic and 3D QSAR approaches in nano-QSAR studies based on biological activity of fullerene derivatives. J. Nanopart. Res. 18, 256.
Kafil, V., Omidi, Y., 2011. Cytotoxic impacts of linear and branched polyethylenimine nanostructures in A431 cells. Bioimpacts 1 (1), 23–30.
Kaur, D., Jain, K., Mehra, N.K., Kesharwani, P., Jain, N.K., 2016. A review on comparative study of PPI and PAMAM dendrimers. J. Nanoparticle Res. 18, 146.
Khan, H.A., Arif, I.A., 2012. Toxic Effects of Nanomaterials. Chapter 1: Nanoparticle-induced Toxicity: Focus on Plants. Bentham E Books, Saudi Arabia.
Kier, L.B., Hall, L.H., 1976. Molecular connectivity. 7. Specific treatment of heteroatoms. J. Pharm. Sci. 65 (12), 1806–1809.
Koper and Borkovec, 2010. Proton binding by linear, branched, and hyperbranched polyelectrolytes. Elsevier 51 (24), 5649–5662.
Labute, P., 2000. A widely applicable set of descriptors. J. Mol. Graph. Model 18 (4–5), 464–477.
Lambert, A., Wagner, M., 2016. Characterisation of nanoplastics during the degradation of polystyrene. Chemosphere 145, 265–268.
Landrum, G., 2016. RDKit: Open-source Chemoinformatics. http://www.rdkit.org.
Lei, C., Zhang, L., Yang, K., Zhu, L., Lin, D., 2016. Toxicity of iron-based nanoparticles to green algae: effects of particle size, crystal phase, oxidation state and environmental aging. Environ. Pollut. 218, 505–512.
Leszczynska, J., Shukla, M., 2009. Practical Aspects of Computational Chemistry: Methods, Concepts and Applications: Chapter 9: Quantitative Structure-activity Relationships (QSARs) in the European REACH System: Could These Approaches Be Applied to Nanomaterials? Springer, Heidelberg, Germany.
Lyklema, J., 2005. Fundamentals of Interface and Colloid Science, vol. 5. Pages 1.1–8.94 Soft Colloids.
Mayo-Bean, K., Morana, K., Meylan, B., Ranslow, P., 2012. Methodology Document for the ECOlogical Structure-activity Relationship Model (ECOSAR) Class Program. USEPA, Washington D.C.
Navarro, E., Baun, A., Behra, R., Hartmann, N., Filser, J., Miao, A.-J., 2008. Environmental behavior and ecotoxicity of engineered nanoparticles to algae, plants, and fungi. Ecotoxicology 17, 372–386.
Netzeva, T., Pavan, M., Worth, A., 2007. Review of Data Sources, QSARs and Integrated Testing Strategies for Aquatic Toxicity. JRC Scientific and Technical Reports. EUR22943EN-2007.
Nolte, T.M., Hartmann, I.B.H., Kleijn, M., Garnæs, J., Van de Meent, D., Hendriks, A.J., Baun, A., 2016. The toxicity of plastic nanoparticles to green algae as influenced by surface modification, medium hardness and cellular adsorption. Aquat. Toxicol. 183, 11–20.
Nolte, T.M., Kettler, K., Meesters, J.A., Hendriks, A.J., van de Meent, D., 2015. A semi-empirical model for transport of inorganic nanoparticles across a lipid bilayer: implications for uptake by living cells. Environ. Toxicol. Chem. 34 (3), 488–496.
Noro, T., 1985. Mechanism of manganese uptake by a green alga, dunaliella tertiolecta butcher. Mem. Fac. Fish. Kagoshima. Univ. 34 (2), 183–244.
OECD, 2011. OECD Guidelines for the Testing of Chemicals, Section 2. Test No. 201: Freshwater Alga and Cyanobacteria, Growth Inhibition Test.
Puzyn, T., Leszczynski, J., Cronin, M.T., 2010. Recent Advances in QSAR Studies: Methods and Applications. Springer, Dordrecht, Netherlands.
Seitz, J.T., 1993. The estimation of mechanical properties of polymers from molecular structure. Appl. Polym. Sci. 49 (8), 1331–1351.
Serin S, Avci H, Polat O. 2013. Sequestering agent used in detergents with high calcium binding capacity. Google Patents EP 2657329 A1. https://www.google.nl/patents/EP2657329A1?cl=en.
Sigrid D, Alexander L, Martina H. 2010. WIPO patent No. WO/2010/069519.
Singh, S.P., Singh, P., 2015. Effect of temperature and light on the growth of algae species: a review. Renew. Sustain. Energy Rev. 50, 431–444.
Tadros, T.F., 2015. Interfacial Phenomena and Colloidal Stability: Basic Principles. De Gruyter, Wokingham, UK.
Tropsha, A., 2010. Best practices for QSAR model development, validation and exploitation. Mol. Inf. 29, 476–488.
Tsuji, J.S., Maynard, A.D., Howard, P.C., James, J.T., Lam, C., Warheit, D.B., Santamariak, A.B., 2006. Research strategies for safety evaluation of nanomaterials, part IV: risk assessment of nanoparticles. Toxicol. Sci. 89 (1), 42–50.
Ullner, M., Jönsson, B., Peterson, C., Sommelius, O., Söderberg, B., 1997. The electrostatic persistence length calculated from Monte Carlo, variational and perturbation methods. J. Chem. Phys. 107 (4).
Uppu, D.S.S.M., Samaddar, S., Hoque, J., Konai, M.M., Krishnamoorthy, P., Shome BR,Haldar, J., 2016. Side chain degradable cationic–amphiphilic polymers with tunable hydrophobicity show in vivo activity. Biomacromolecules 17 (9), 3094–3102.
US EPA, 2012. Estimation Programs Interface Suite™ for Microsoft® Windows, V. 4.11. United States Environmental Protection Agency, Washington, DC, USA.
US EPA, 2013. Interpretive Assistance Document for Assessment of Polymers. Sustainable Futures Summary Assessment. United States Environmental Protection Agency, Washington, DC, USA.
Van Hoecke, K., De Schamphelaere, K.A., Van der Meeren, P., Lucas, S., Janssen, C.R., 2008. Ecotoxicity of silica nanoparticles to the green alga Pseudokirchneriella subcapitata: importance of surface area. Environ. Toxicol. Chem. 27 (9), 1948–1957.
Van Hoecke, K., Quik, J.T.K., Mankiewicz-Boczek, J., De Schamphelaere, K.A.C., Elsaesser, A., Van der Meeren, P., Barnes, C., McKerr, G., Howard, C.V., Van De Meent, D., Rydzyński, K., Dawson, K.A., Salvati, A., Lesniak, A., Lynch, I., Silversmit, G., De Samber, B., Vincze, L., Janssen, C.R., 2009. Fate and effects of CeO2 nanoparticles in aquatic ecotoxicity tests. Environ. Sci. Technol. 43 (12), 4537–4546.
Van Hoecke, K., De Schamphelaere, K.A.C., Van der Meeren, P., Smagghe, G., Janssen, C.R., 2011. Aggregation and ecotoxicity of CeO2 nanoparticles in synthetic and natural waters with variable pH, organic matter concentration and ionic strength. Environ. Pollut. 159, 970–976.
van Hoecke, K., De Schamphelaere, K.A.C., Ali, Z., Zhang, F., Elsaesser, A., Rivera-Gil, P., Parak, W.J., Smagghe, G., Howard, C.V., Janssen, C.R., 2013. Ecotoxicity and uptake of polymer coated gold nanoparticles. Nanotoxicology 7 (1), 37–47.
Verbruggen, E.M.J., 2012. Environmental Risk Limits for Polycyclic Aromatic Hydrocarbons (PAHs) for Direct Aquatic, Benthic, and Terrestrial Toxicity. RIVM report 607711007/2012.
Volgusheva, A., Kukarskikh, G., Krendeleva, T., Rubina, A., Mamedov, F., 2015. Hydrogen photoproduction in green algae Chlamydomonas reinhardtii under magnesium deprivation. RSC Adv. 5, 5633.
von Moos, N., Slaveykova, V.I., 2014. Oxidative stress induced in bacteria and aquatic microalgae – state of the art and knowledge gaps. Nanotoxicology 8 (6), 605–630.
Wildman, S.A., Crippen, G.M., 1999. Prediction of physicochemical parameters by atomic contributions. J. Chem. Inf. Comput. Sci. 39, 868–873.
Wilson, A.D., Nicholson, J.W., 1993. Acid-base Cements: Their Biomedical and Industrial Applications. Chapter 4: Polyeletrolytes, Ions Binding and Gelation. Cambridge University Press, Cambridge, UK.
Yachandra, V.K., Yano, J., 2011. Calcium in the oxygen-evolving complex: structural and mechanistic role determined by X-ray spectroscopy. J. Photochem. Photobiol. B Biol. 104 (1–2), 51–59.
Young, R.J., Lovell, P.A., 2011. Introduction to Polymers, third ed. CRC Press, Boca Raton, FL.
Zamani, H., Moradshahi, A., Jahromi, H.D., Sheikhi, M.H., 2014. Influence of PbS nanoparticle polymer coating on their aggregation behavior and toxicity to the green algae Dunaliella salina. Aquat. Toxicol. 154, 176–183.